THE JOURNAL OF BIOLOGICAL CHEMISTRY VOL. 290, NO. 11, pp. 6925–6936, March 13, 2015

Evidence of a Structural and Functional Ammonium Transporter RhBG·Anion Exchanger 1·Ankyrin-G Complex in Kidney Epithelial Cells*

Received for publication, September 8, 2014, and in revised form, January 12, 2015 Published, JBC Papers in Press, January 23, 2015, DOI 10.1074/jbc.M114.610048

Sandrine Genetet[‡§¶‖], Pierre Ripoche[‡§¶‖], Caroline Le Van Kim[‡§¶‖], Yves Colin[‡§¶‖1], and Claude Lopez[‡§¶‖1,2]

From [‡]INSERM U1134, 75739 Paris, France, the [§]Université Paris Diderot, Sorbonne Paris Cité, UMR_S1134, 75739 Paris, France, the [¶]Institut National de la Transfusion Sanguine, 75739 Paris, France, and the [‖]Laboratoire d'Excellence GR-Ex, 75238 Paris, France

Background: Up to now, there was no evidence for an interaction of the kidney anion exchanger 1 (kAE1) with ankyrin.
Results: kAE1 actually associates with epithelial ankyrin-G and renal ammonium transporter RhBG, which also binds ankyrin-G.
Conclusion: RhBG, kAE1 and ankyrin-G form a structural/functional complex in kidney epithelial cell lines.
Significance: This complex could participate in the regulation of acid-base homeostasis.

The renal ammonium transporter RhBG and anion exchanger 1 kAE1 colocalize in the basolateral domain of α-intercalated cells in the distal nephron. Although we have previously shown that RhBG is linked to the spectrin-based skeleton through ankyrin-G and that its NH_3 transport activity is dependent on this association, there is no evidence for an interaction of kAE1 with this adaptor protein. We report here that the kAE1 cytoplasmic N terminus actually binds to ankyrin-G, both in yeast two-hybrid analysis and by coimmunoprecipitation *in situ* in HEK293 cells expressing recombinant kAE1. A site-directed mutagenesis study allowed the identification of three dispersed regions on kAE1 molecule linking the third and fourth repeat domains of ankyrin-G. One secondary docking site corresponds to a major interacting loop of the erythroid anion exchanger 1 (eAE1) with ankyrin-R, whereas the main binding region of kAE1 does not encompass any eAE1 determinant. Stopped flow spectrofluorometry analysis of recombinant HEK293 cells revealed that the Cl^-/HCO_3^- exchange activity of a kAE1 protein mutated on the ankyrin-G binding site was abolished. This disruption impaired plasma membrane expression of kAE1 leading to total retention on cytoplasmic structures in polarized epithelial Madin-Darby canine kidney cell transfectants. kAE1 also directly interacts with RhBG without affecting its surface expression and NH_3 transport function. This is the first description of a structural and functional RhBG·kAE1·ankyrin-G complex at the plasma membrane of kidney epithelial cells, comparable with the well known Rh·eAE1·ankyrin-R complex in the red blood cell membrane. This renal complex could participate in the regulation of acid-base homeostasis.

Erythroid anion exchanger 1 (eAE1),[3] also known as Band 3, is the major integral membrane protein of the red blood cell (RBC). This glycoprotein of 911 amino acids consists of three distinct regions: (i) an N-terminal cytoplasmic domain (404 residues) that binds various glycolytic enzymes, protein tyrosine kinases and hemoglobin, as well as cytoskeletal proteins such as bands 4.1 and 4.2, and ankyrin-R; (ii) a membrane multi-spanning domain (467 residues) mediating the electroneutral chloride/bicarbonate (Cl^-/HCO_3^-) exchange function; and (iii) a short C-terminal cytoplasmic domain (40 residues) that binds carbonic anhydrase II to form a functional metabolon (3). By its association with proteins Rh, the carrier of the Rhesus blood group antigens, and RhAG, which define the core of the Rh membrane complex, eAE1 modulates their expression level (4). RhAG belongs to the ammonium transporters/methylammonium-ammonium permease/Rh superfamily of ammonium transporters and allows the facilitated transport of NH_3 across the RBC membrane (5). Ankyrin-R mediates skeleton attachment of Rh and RhAG (6); therefore an Rh·eAE1 macrocomplex model has been proposed (4) in which the Rh complex and eAE1 are associated with each other and the spectrin-based skeleton through their common direct interaction with ankyrin-R (6). The Rh·eAE1·ankyrin-R macrocomplex could constitute a metabolon allowing transport of gas and/or ions across the RBC membrane (4).

The kidney isoform of AE1 (kAE1) is identical to eAE1, except that it lacks the N-terminal 65 amino acids because of an alternate transcription start site (7). kAE1 is located in the basolateral domain of the acid-secreting α-intercalated cells of the distal tubule (8), where it plays an important role in bicarbonate reabsorption into the blood and in urinary acidification. Mutations of kAE1 are responsible for dominant or recessive distal renal tubular acidosis, which results in impaired acid secretion

* This work was supported by institutional funding to the INSERM U1134 and Institut National de la Transfusion Sanguine. This study was supported by Laboratory of Excellence GR-Ex Grant ANR-11-LABX-0051. The labex GR-Ex is funded by the program Investissements d'Avenir of the French National Research Agency through Grant ANR-11-IDEX-0005-02.
[1] These authors contributed equally to this work.
[2] To whom correspondence should be addressed: INSERM, UMR_S1134, INTS, 6 Rue Alexandre Cabanel, 75015 Paris, France. Tel.: 33-1-44-49-30-95; Fax: 33-1-43-06-50-19; E-mail: claude.lopez@inserm.fr.

[3] The abbreviations used are: AE1, type 1 anion exchanger; eAE1, erythroid AE1; kAE1, kidney AE1; Rh, Rhesus; Nter, N terminus; RBC, red blood cell; MDCK, Madin-Darby canine kidney; PLA, proximity ligation assay; BCECF-AM, 2′,7′bis-(2-carboxyethyl)-5(6)-carboxyfluorescein acetoxymethyl ester; DIDS, 4,4′-diisothiocyanatostilbene-2,2′-disulfonic acid, disodium salt; ni, noninduced; i, induced.

(3). In α-intercalated cells, kAE1 is colocalized with the basolateral ammonium transporter RhBG (9, 10), a renal homologue of the erythroid RhAG protein (11). We have previously shown that RhBG is tethered to the membrane skeleton through its interaction with ankyrin-G (1) and that this linkage is crucial for its NH_3 transport activity (2). Ankyrins constitute a family of membrane adaptor proteins that link various membrane-associated proteins (ion channels and cell adhesion molecules) to the spectrin-based membrane skeleton. In vertebrates, three different genes *Ank1*, *Ank2*, and *Ank3* encode ankyrin-R, ankyrin-B, and ankyrin-G, respectively. Ankyrin-R expression is restricted to erythrocytes, neurons, and striated muscle; ankyrin-B is broadly expressed and represents the major form in the nervous system; ankyrin-G is the most widely distributed species and is predominant in epithelial cells. These last two forms are not found in red cells (12, 13). Two past studies from 1994 (14) and 1995 (15) reported that the kAE1 isoform does not bind ankyrin *in vitro*; however, ankyrin-G was still not characterized at that time, and these experiments were achieved using ankyrin-R, which is not found in kidney epithelial cells. The crystal structure of the N-terminal cytoplasmic domain (Nter) of eAE1, although not resolving the first 54 amino acids, showed that the absence of residues 1–65 in kAE1 results in a deletion of a central strand in the major β-sheet. The authors assumed that this deletion might cause the loss of interaction between kAE1-Nter and ankyrin, protein 4.1, and glycolytic enzymes (16). A comparative biophysical analysis of cytoplasmic domains of eAE1 and kAE1 concluded that the absence of the central β-strand in the latter results in a less stable and more open structure than that of eAE1 and may account in part for the altered protein binding properties of kAE1-Nter (17). Despite these presumptions, there is so far no experimental evidence of the absence of interaction between kAE1 and the epithelial form of ankyrin, ankyrin-G.

We made the hypothesis that, similarly to erythroid Rh·eAE1·ankyrin-R, a RhBG·kAE1·ankyrin-G complex might be present at the plasma membrane of kidney epithelial cells. In this study, we demonstrate the existence of a physical interaction between kAE1 and ankyrin-G and also between kAE1 and RhBG. Moreover, ankyrin-G binding might be crucial for the activities of the membrane partners in this complex: RhBG and kAE1. This newly characterized RhBG·kAE1·ankyrin-G complex could participate in the regulation of acid/base homeostasis by excreting ammonium and protons in urine.

EXPERIMENTAL PROCEDURES

Materials—Primers used in PCR and mutagenesis experiments were from Eurofins MWG/Operon (Ebersberg, Germany). The QuikChange II XL site-directed mutagenesis kit was provided by Stratagene (La Jolla, CA). The pGBKT7 and pGADT7 vectors were from the Matchmaker Gal4 two-hybrid System 3 (Clontech). The pcDNA4/TO-pcDNA6/TR (T-REx™ System) vectors were purchased from Invitrogen. BCECF-AM fluorescent probe and AE1 inhibitor DIDS were obtained from Sigma-Aldrich. Mouse BRIC 6 and rat BRAC 17 monoclonal antibodies to extracellular epitopes of human AE1 were provided by the International Blood Group Reference Laboratory (Bristol, UK). Rabbit polyclonal antiserum against the cytoplasmic N terminus of AE1 was a gift from Dr. Carsten Wagner (University of Zürich, Zürich, Switzerland). Rabbit and A-08 mouse polyclonal antibodies raised against, respectively, the cytoplasmic C terminus and extracellular loops of human RhBG have been described previously (1, 2, 18). Mouse anti-human ankyrin-G and anti-ZO-1 (Alexa Fluor 488-conjugated) monoclonal antibodies were purchased from Invitrogen and Molecular Probes (Saint-Aubin, France), respectively. Complete protease inhibitor mixture was supplied by Roche Applied Science.

Yeast Two-hybrid Studies—The pGADT7 constructs containing the four individual D1, D2, D3, and D4 sequences coding for the repeat subdomains of the membrane binding domain of ankyrin-G, fused to GAL4 activation domain cDNA, were previously described (1). A cDNA fragment encoding the cytoplasmic N-terminal domain of kAE1 (kAE1-Nter, residues 1–339, starting from the kAE1-specific ATG codon) was amplified by PCR from the plasmid pUC18-eAE1 containing the erythroid AE1 coding sequence and cloned in the pGBKT7 vector in-frame with the DNA binding domain of GAL4. Mutant forms of kAE1-Nter were obtained by site-directed mutagenesis according to the supplier's instructions (Stratagene) or PCR amplification from pGBKT7-kAE1-Nter recombinant DNA or by gene synthesis by Eurofins MWG/Operon. All the inserts were sequenced by GATC Biotech (Konstanz, Germany). Cotransformation of the AH109 yeast strain with pGBKT7 and pGADT7 constructs and analysis of protein interactions were carried out as described previously (1).

Construction of kAE1 Mammalian Expression Vectors—Full-length cDNA encoding kAE1 was amplified by PCR from the plasmid pUC18-eAE1 with the addition of a Kozak sequence at its 5′ end and subcloned in the pcDNA4/TO vector. The kAE1 cDNA lacking coding sequences necessary for interaction with ankyrin-G was synthesized by Eurofins MWG/Operon and then subcloned in the pcDNA4/TO vector. All the inserts were sequenced by GATC Biotech.

Cell Culture, Transfection, Flow Cytometry, and Confocal Microscopy—HEK293 cells and Madin-Darby canine kidney (MDCK) cells were supplied by the American Type Culture Collection (Manassas, VA). HEK293 cells were grown in Dulbecco's modified Eagle's medium/F12/GlutaMAX I (Invitrogen) supplemented with 10% (v/v) fetal calf serum tetracycline-free (Dutscher, Brumath, France), 1× nonessential amino acids (Invitrogen), 1× antibiotic-antimycotic (Invitrogen), 25 mM $NaHCO_3$, and 25 mM Hepes, and MDCK cells were cultured in Iscove's modified Dulbecco's medium/GlutaMAX I (Invitrogen) supplemented with 10% fetal calf serum and antibiotic-antimycotic. T-REx (Invitrogen) is a Tet-regulated mammalian expression system based on the binding of tetracycline to a Tet repressor and derepression of the promoter controlling the expression of the gene of interest. The establishment of a HEK293 cell line inducible for expression of recombinant kAE1 protein was achieved as described previously for recombinant eAE1 expression (19). In kAE1-RhBG coexpression experiments, HEK293 stable transfectants (pcDNA6/TR + pcDNA4/TO-kAE1) were cotransfected with pcDNA3-RhBG vector (1) and selected using 0.8 mg/ml neomycin (Geneticin; Invitrogen). Surface expression of kAE1 and RhBG on HEK293 cells was detected by flow cytometry, using a FACSCanto II flow cytometer (BD Bio-

sciences), after staining with mouse monoclonal BRIC 6 (1:40) and mouse polyclonal A-08 (1:200), respectively, as primary antibodies, and goat anti-mouse fluorescein isothiocyanate or phycoerythrin-conjugated F(ab′)2 fragments (Beckman Coulter) (1:100), respectively, as secondary antibodies. For immunofluorescence experiments, HEK293 stable transfectants were cultured on poly-L-lysine coverslips (BD Biosciences). Cells were induced or not for kAE1 expression, fixed, permeabilized or left untreated, immunostained with appropriate primary and Alexa Fluor secondary antibodies as described previously (19), and examined by confocal microscopy using a Zeiss LSM700 inverted confocal microscope equipped with a ×100 oil immersion objective with a numerical aperture of 1.4. MDCK cells grown to subconfluency on poly-L-lysine coverslips were transiently transfected with pcDNA4/TO-kAE1 vector using TurboFect transfection reagent (Thermo Scientific, St. Leon-Rot, Germany), cultured for 4 days to allow polarization, immunostained with appropriate primary and Alexa Fluor secondary antibodies, and analyzed by confocal microscopy.

Proximity Ligation Assay—Proximity ligation assay (PLA) was used for *in situ* detection of protein interactions. HEK293 cells expressing recombinant proteins were cultured on coverslips, induced or not for kAE1 expression as above, fixed with 4% paraformaldehyde (w/v), permeabilized in 1% SDS (w/v), and blocked with background reducing buffer (Dako, Copenhagen, Denmark), as described previously (1). Then the samples were incubated for 1 h at room temperature with the following pairs of antibodies, according to the interaction studied: rabbit anti-AE1 (1:4000) and mouse anti-ankyrin-G (10 μg/ml) for kAE1-ankyrin-G, rabbit anti-RhBG (1:500), and mouse anti-ankyrin-G (10 μg/ml) for RhBG-ankyrin-G. PLA was performed in a humid chamber at 37 °C according to the manufacturer's instructions (Olink Bioscience, Uppsala, Sweden). Briefly, after three washings in buffer A, the samples were incubated with mouse plus and rabbit minus PLA probes and washed again, and ligation mixture was then added for 30 min. Washings were repeated, and the samples were finally incubated for 100 min with the amplification mixture containing the fluorescently labeled DNA probe, washed in buffer B, mounted in ProLong Gold antifade reagent with DAPI (Invitrogen), and analyzed by confocal microscopy. For kAE1-RhBG interaction, samples (not permeabilized) were incubated with mouse A-08 anti-RhBG (1:3000) and rat BRAC17 anti-AE1 (4 μg/ml) conjugated with minus PLA probe (according to Olink's instructions for Probemaker kit), followed by the mouse plus PLA probe and then treated as above. A positive signal indicating an interaction is produced when the two tested proteins are ≤30 nm apart.

Protein Extraction, Electrophoresis and Western Blot Analysis—HEK293 cell lines were lysed for 1 h at 4 °C in lysis buffer (150 mM NaCl, 20 mM Tris-HCl, pH 8, 5 mM EDTA) containing complete protease inhibitor mixture and 1% Triton X-100. Lysates were centrifuged at 15,000 × *g* for 15 min at 4 °C. Aliquots of lysate supernatants were mixed with 5× loading buffer (1.25 mM sucrose, 20% SDS, 250 mM Tris-HCl, pH 6.8, 25% β-mercaptoethanol, 1% bromphenol blue) before electrophoresis. SDS-PAGE was performed using 4–12% gradient polyacrylamide gels according to Laemmli (20), using MOPS SDS running buffer (Novex, Saint-Aubin, France). Western blots were performed on nitrocellulose membranes which then were incubated with rabbit anti-AE1 antibody (1:10,000) followed with anti-rabbit IgG peroxidase-conjugated secondary antibody (1:1,000) (P.A.R.I.S., Compiègne, France). Immunoblots were visualized using the ECL Plus Western blotting detection system (Amersham Biosciences).

Stopped Flow Analysis—Ammonium transport (RhBG) and Cl^-/HCO_3^- exchange (kAE1) functions were determined by stopped flow spectrofluorometry analysis using the fluorescent pH-sensitive probe BCECF-AM (10 μM) at pH 7.2, essentially as described previously (10, 19). Briefly, parental and transfected HEK293 cells were exposed either to an outwardly directed 20 mEq NH_4^+ at 15 °C (ammonium transport) or to inwardly directed 10 meq HCO_3^-/CO_2 and outwardly directed 67.5 meq Cl^- gradients at 30 °C (Cl^-/HCO_3^- exchange). When indicated, the anion transport inhibitor DIDS was added to the cells at 10 μM 30 min before analysis. The pH-dependent fluorescence changes of BCECF were monitored at a 485-nm excitation wavelength, and the emitted light was filtered with a 520-nm cutoff filter. Data from three to four time courses were averaged and fitted to a monoexponential function using the simplex procedure of the Biokine software package (Bio-Logic). Determined alkalinization rate constants could be compared in the different samples because cell sizes were identical in all preparations. They represent a reliable indication of transport functions because in each case, NH_3 or HCO_3^- movements result in pH modification with always the same buffer power. Over the pH range used (7.0–7.8), the relative fluorescence of the dye was proportional to the pH variation ($R^2 = 0.993$), as determined by titration of HEK293 cells incubated in 2 ml of isotonic buffer (130 mM NaCl, 5 mM KCl, 10 mM Hepes/NaOH, pH 7.2) containing 1 μM valinomycin and 1 μM carbonyl cyanid 4-(trifluoromethoxy phenylhydrazone) (Sigma-Aldrich). Titrations were performed using a classical spectrofluorimeter by stepwise additions of 2 μl of 1 N KOH.

RESULTS

Interaction of kAE1 with Ankyrin-G in Yeast Two-hybrid Analysis—eAE1 interacts with ankyrin-R through its cytoplasmic N terminus (3). To investigate whether the nonerythroid and epithelial homologue ankyrin-G could be a partner of kAE1, the N-terminal cytoplasmic tail of kAE1 (kAE1-Nter) was fused in-frame to the GAL4 DNA binding domain of the yeast two-hybrid pGBKT7 vector. The four repeat domains of ankyrin-G (D1, D2, D3, and D4) individually fused in-frame to the GAL4 activation domain of the pGADT7 vector were already available (1). The recombinant vectors were cotransformed in the AH109 yeast strain, and their ability to grow in high stringency selective medium lacking adenine, histidine, leucine, and tryptophan was analyzed (Fig. 1*A*). These experiments, confirmed by β-galactosidase activity assays (not shown), indicated that kAE1-Nter interacts with the D3 and D4 repeat domains of ankyrin-G. No association between kAE1-Nter and the D1 and D2 repeat domains could be detected.

Mapping of the Ankyrin-G-Binding Site in the Cytoplasmic N Terminus of kAE1—We next performed site-directed mutagenesis on the pGBKT7-kAE1-Nter vector to localize the site of

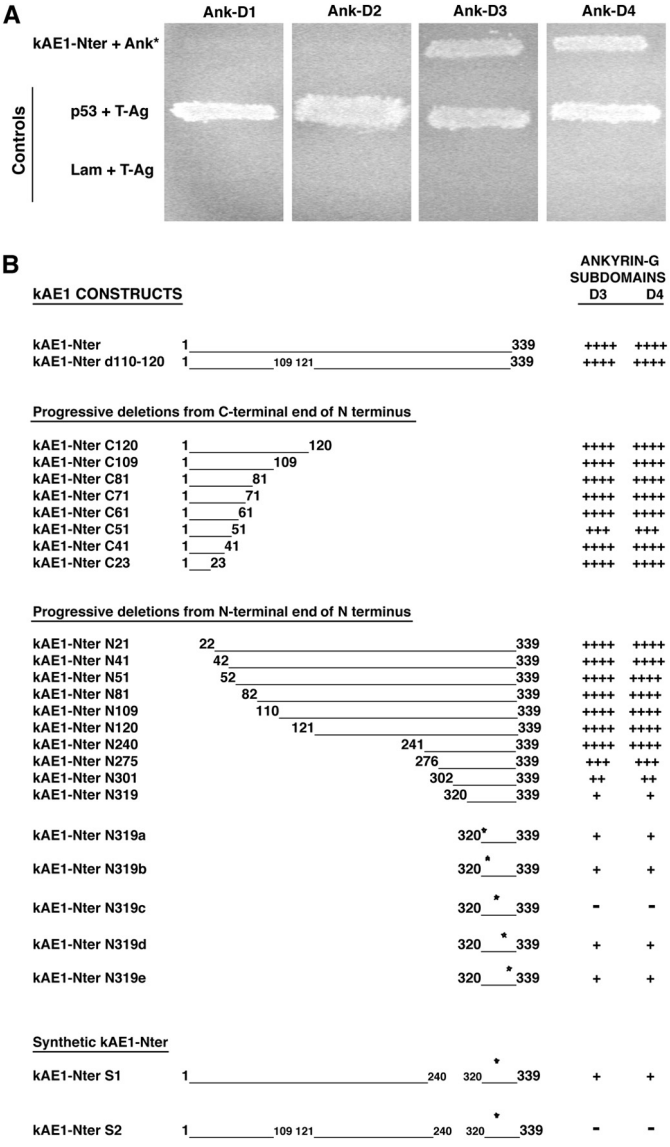

FIGURE 1. **Yeast two-hybrid analysis of the interaction between kAE1 and ankyrin-G.** *A*, interaction of wild-type cytoplasmic N terminus of kAE1 (*kAE1-Nter*) with the membrane binding domain of ankyrin-G. The four repeat subdomains Ank-D1, Ank-D2, Ank-D3, and Ank-D4 of the membrane binding domain of ankyrin-G cloned in the pGADT7 vector were tested for their ability to interact with kAE1-Nter cloned in the pGBKT7 vector in the yeast two-hybrid system. The ability of cotransformed yeast to grow on selective medium lacking adenine, histidine, leucine, and tryptophan indicated a specific interaction of kAE1-Nter with D3 and D4 domains of ankyrin-G. The previously described interaction between the large T-antigen of SV40 (*T-Ag*) and murine p53 (50) was used as positive control. As negative control, human lamin C (*Lam*) and T-antigen (51) were used. For each cotransformation, three colonies were streaked on selective media. *Ank-D** is for Ank-D1, Ank-D2, Ank-D3, or Ank-D4. *B*, mapping of the ankyrin-G binding site of kAE1. *Left* and *middle panels*, schematic representation of wild-type (*kAE1-Nter*) and different mutant cytoplasmic N termini of kAE1. Internal deletion (*kAE1-Nter d110–120*), progressive deletions from the C-terminal end of the N terminus (*kAE1-Nter C120* to *C23*) or the N-terminal end of the N terminus (*kAE1-Nter N21* to *N319*), and alanine substitutions of 4-amino acid stretches (*kAE1-Nter N319a* to *N319e*) were generated from kAE1-Nter in the pGBKT7 vector, as described under "Results." kAE1-Nter S1 and S2 were created by synthesis of mutant kAE1 cDNAs (see "Results") and cloning in pGBKT7. *, location of alanine substitutions in kAE1 mutants (D320A/I321A/R322A/R323A, R324A/Y325A/P326A/Y327A, Y328A/L329A/S330A/D331A, I332A/T333A/D334A/A335, and F336A/S337A/P338A/Q339A in *kAE1-Nter N319a*, *N319b*, *N319c*, *N319d*, and *N319e* mutants, respectively; Y328A/L329A/S330A/D331A in *kAE1-Nter S1* and *S2* mutants). *Right panel*, results of two-hybrid assays performed as in *A*. The ability of yeast cotransformed by the different mutant pGBKT7-kAE1 vectors and pGADT7-D3 or D4 vectors (*Ankyrin-G subdomains D3* and *D4*) to grow on selective media and to produce β-galactosidase activity was compared with that of wild-type cotransformants. ++++, interaction equivalent to wild-type kAE1 with D3 and D4 subdomains; +++, ++, and +, interaction slightly, moderately, and drastically decreased, respectively; −, no interaction.

interaction with the D3 and D4 repeat domains of ankyrin-G, using the two-hybrid system. First, the deletion of the D3-D4 ankyrin-R binding site in eAE1 protein (amino acids 175–185; Ref. 21) was achieved (amino acids 110–120 in kAE1 numbering). The deleted 11 residues were substituted with a bridging Gly-Gly dipeptide, as originally done by Chang and Low (21) on eAE1. Analysis of growth on selective medium and β-galactosidase activity of cotransformed yeast showed a strong interaction of kAE1-Nter d110–120 mutant with D3 and D4 repeat domains of ankyrin-G, apparently equivalent to that of wild-type N terminus of kAE1 (kAE1-Nter) (Fig. 1*B*), indicating that ankyrin-G binding site in kAE1-Nter might be different from ankyrin-R binding site in eAE1-Nter. We then generated a series of mutants with progressive deletions from the C-terminal end of the N terminus, by introduction of stop codons after codons 120, 109, 81, 71, 61, 51, 41, and 23 (positions in kAE1 protein), respectively (Fig. 1*B*, series *kAE1-Nter C*). Surprisingly, none of these mutants exhibited a decrease of interaction with ankyrin-G, except a mild diminution for C51, but not for the shortest C41 and C23 mutants. To address this issue, progressive deletions from the N-terminal end of the N terminus (N21, N41, N51, N81, N109, N120, N240, N275, N301, and N319) were performed by PCR-amplifying kAE1-Nter fragments starting at codons 22, 42, 52, 82, 110, 121, 241, 276, 302, and 320, respectively (Fig. 1*B*). No modification of interaction with ankyrin-G was observed from N21 to N240 mutants; this suggests that the full interaction still detected with the C-terminal mutants (from C120 to C23) was most probably artifactual and caused by a modified conformation of these short peptides. From N275 to N319 mutants, interaction with ankyrin-G was progressively reduced but not completetely inhibited (Fig. 1*B*). Alanine scanning on the N319 mutant was then performed, by stretches of four amino acids (D320A/I321A/R322A/R323A = *N319a*, R324A/Y325A/P326A/Y327A = *N319b*, Y328A/L329A/S330A/D331A = *N319c*, I332A/T333A/D334A/A335 = *N319d*, and F336A/S337A/P338A/Q339A = *N319e*; Fig. 1*B*). N319a, N319b, N319d, and N319e mutants were not further affected in their capacity to bind ankyrin-G, compared with N319, whereas the interaction of N319c mutant with ankyrin-G was completely abolished. However, this short mutant lacks the 240 first amino acids of full-length kAE1-Nter, spatial conformation of which might be important for the interaction. A synthetic N terminus was therefore created that contained both a deletion between amino acids 240 and 320 and the four substitutions Y328A/L329A/S330A/D331A. Two-hybrid experiments showed that this kAE1-Nter S1 mutant still interacted with ankyrin-G, at the same level as the N319 mutant (Fig. 1*B*). However, the introduction of the d110–120 deletion in the S1 mutant led to a complete inhibition of its binding to D3 and D4 repeat domains of ankyrin-G (Fig. 1*B*, *kAE1-Nter S2*). These 11 residues therefore contribute to interaction with ankyrin-G only as a second-

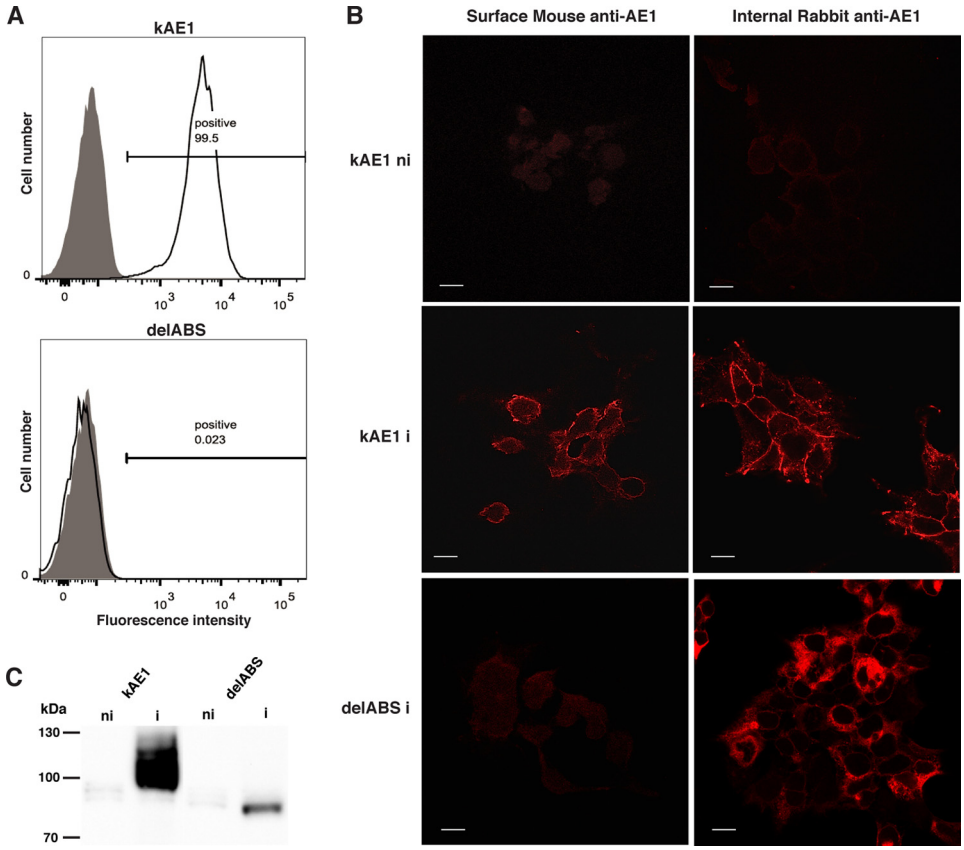

FIGURE 2. **Expression of recombinant kAE1 protein in HEK293 cell transfectants.** *A*, flow cytometry analysis of wild-type and delABS kAE1 surface expression using BRIC6 monoclonal antibody. *Gray* and *white peaks*, noninduced and induced cells for kAE1 expression, respectively. Percentages of positive transfected cells are indicated. *B*, immunofluorescence confocal microscopy analysis. HEK293 transfected cells were cultured on poly-L-lysine coverslips, tetracycline-induced for kAE1 expression, and fixed in 4% paraformaldehyde. *Left panels*, cells were directly labeled with mouse anti-AE1 BRIC6 primary antibody and Alexa Fluor 568 goat anti-mouse IgG secondary antibody. *Right panels*, cells were permeabilized in 1% SDS before staining with rabbit anti-AE1 and Alexa Fluor 568 goat anti-rabbit IgG. *kAE1 ni*, noninduced HEK293-kAE1 cells; *kAE1 i*, induced HEK293-kAE1 cells; *delABS i*, induced HEK293-kAE1-delABS cells. *Scale bars*, 15 μm. *C*, immunoblot of wild-type and delABS kAE1 proteins extracted from HEK293 transfected cells using rabbit anti-AE1 antibody.

ary domain. The ankyrin-G binding site is thus dispersed on three distinct regions in the N terminus of kAE1: amino acids 110–120, 241–319, and 328–331.

Expression of Recombinant Wild-type and Mutant kAE1 in HEK293 Cells—We constructed a synthetic cDNA encoding a whole kAE1 protein lacking in its cytoplasmic N terminus the two peptidic regions (amino acids 110–120 and 241–319) and with alanine substitutions for residues 328–331, named kAE1-delABS (deletion of ankyrin-G binding site) and thus identical to kAE1-Nter S2 mutant in its cytoplasmic N terminus. HEK293 cells, lacking endogenous expression of kAE1 (22), were stably transfected with wild-type or mutant kAE1 cDNA using the tetracycline-inducible expression system previously described (19) to circumvent the loss of long term expression of AE1 protein (23, 24). Flow cytometry experiments using BRIC6 antibody revealed wild-type kAE1 at the surface of tetracycline-induced transfected cells (Fig. 2*A*, *kAE1*, *white peak*). More than 99% of the transfected cells expressed kAE1 protein after Zeocin selection and cell sorting. As expected, no labeling could be detected either on parental HEK293 cells (not shown) or on noninduced kAE1-transfected cells (Fig. 2*A*, *kAE1*, *gray peak*). Likewise, the delABS mutant was not revealed at the cell surface (Fig. 2*A*, *delABS*, superimposed *gray* and *white peaks*). Immunofluorescence confocal microscopy on intact cells using BRIC6 confirmed these results (Fig. 2*B*, *middle* and *lower left panels*): wild-type kAE1 was localized on the cell surface, whereas kAE1-delABS was not detectable. The same result was obtained when using BRAC17, another exofacial epitope-recognizing antibody (not shown). After cell permeabilization, wild-type kAE1 was located almost exclusively at the cell membrane, whereas kAE1-delABS mainly accumulated on cytoplasmic structures and was partly detectable at the plasma membrane, using anti-Nter AE1 antibody (Fig. 2*B*, *middle* and *lower right panels*). kAE1 was not expressed in parental (not shown) or noninduced transfected cells (*kAE1 ni*; Fig. 2*B*, *top panels*). Western blot analysis of Triton X-100 solubilized HEK293 cell proteins revealed that wild-type kAE1 and kAE1-delABS migrate in SDS-PAGE at an estimated apparent molecular mass of 93 and 83 kDa, respectively, as expected (Fig. 2*C*), which rules out an altered synthesis or stability of the mutant protein. kAE1-delABS therefore is not efficiently trafficked to the plasma membrane and might also display a defect of folding that would explain failure to detect the protein at the surface of intact cells.

Interaction of kAE1 and RhBG with Ankyrin-G in Proximity Ligation Assay—To strengthen the data of kAE1 interaction with ankyrin-G from two-hybrid experiments, we performed PLA in recombinant HEK293 cells. This *ex vivo* coimmunoprecipitation allows the detection of protein-protein interactions

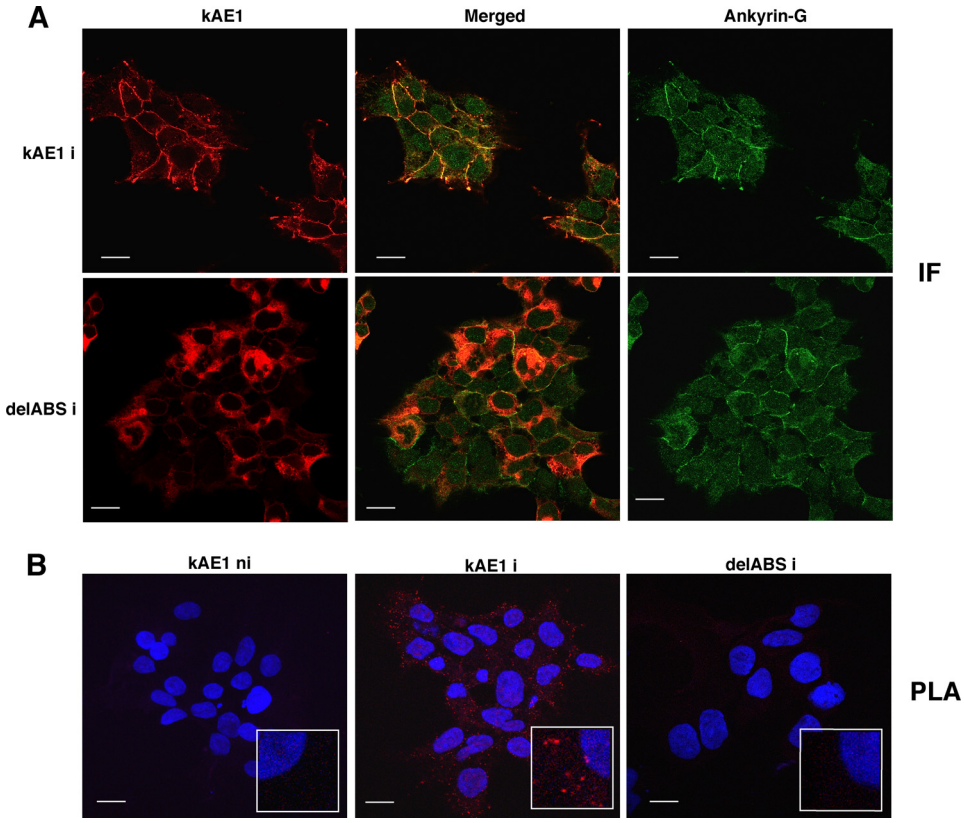

FIGURE 3. **Analysis of the interaction between kAE1 and ankyrin-G by coimmunoprecipitation *in situ*.** *A*, colocalization of recombinant kAE1 with endogenous ankyrin-G. HEK293 transfected cells grown on poly-L-lysine coverslips and tetracycline-induced for wild-type (*kAE1 i*) or delABS (*delABS i*) kAE1 expression were fixed and permeabilized as in Fig. 2, stained with rabbit anti-AE1 (*kAE1*, *red*) and mouse anti-ankyrin-G (*Ankyrin-G*, *green*), then stained with Alexa Fluor 568 anti-rabbit and Alexa Fluor 488 anti-mouse IgG, respectively, and analyzed by confocal microscopy. *Merged*, overlay of kAE1 and ankyrin-G immunofluorescence (*IF*) signals. *B*, interaction of kAE1 with ankyrin-G. The same cells grown on poly-L-lysine coverslips were either tetracycline-induced (*i*) or noninduced (*ni*), treated, and stained with primary antibodies as in *A* and then subjected to PLA analysis. Samples were mounted in ProLong Gold antifade reagent with DAPI, allowing cell nuclei staining. The *red* PLA signal was clearly visible in cells expressing wild-type kAE1 (*kAE1 i*) and absent in those expressing kAE1-delABS (*delABS i*) or noninduced for kAE1 expression (*kAE1 ni*). *Inset*, magnification (×16) of a selected region of PLA image. *Scale bars*, 15 μm.

in situ without altering the cellular environment, with a distance resolution of ≤30 nm (25). Preliminary immunofluorescence experiments showed that wild-type kAE1 colocalized with endogenous ankyrin-G (Fig. 3*A*). The delABS mutant partially colocalized with this adaptor protein (Fig. 3*A*, *delABS i*, *Merged*) and showed an essentially submembraneous and internal pattern of expression (by comparison with ankyrin-G expression). This observation attested that at least some protein could reach and tether to the plasma membrane. PLA signal (Fig. 3*B*) was clearly revealed in HEK293 cells expressing recombinant kAE1 (tetracycline-induced) and endogenous ankyrin-G (*kAE1 i*), whereas no signal was visible either in noninduced transfected cells (*kAE1 ni*) or in induced cells transfected with eAE1 cDNA (not shown). Thus kAE1 does interact with ankyrin-G, and as expected, eAE1 (which binds erythroid ankyrin-R) does not. Although kAE1-delABS partially colocalized with ankyrin-G, no signal could be detected by PLA (Fig. 3*B*, *delABS i*), indicating an absence of interaction, as found in two-hybrid experiments. We have previously demonstrated by yeast two-hybrid analysis, immunohistochemistry on kidney epithelial tissue, and immunofluorescence on polarized MDCK cells that RhBG interacts with ankyrin-G (1). Colocalization of both proteins was checked in HEK293 cells expressing either wild-type RhBG or RhBG-F419A/L420A/D421A mutant (binding or not binding, respectively, to ankyrin-G; Ref. 1) (Fig. 4*A*). PLA performed on these cells showed a bright signal with wild-type RhBG, whereas none was visible with the mutant RhBG-F419A/L420A/D421A protein (Fig. 4*B*), which confirmed the binding of wild-type RhBG, but not of RhBG-F419A/L420A/D421A, to ankyrin-G.

Interaction of RhBG with kAE1 in Proximity Ligation Assay—To search for a potential direct interaction between RhBG and kAE1, HEK293 cells expressing inducible wild-type kAE1 or delABS mutant were stably cotransfected with wild-type or F419A/L420A/D421A RhBG cDNA. Confocal microscopy revealed that RhBG colocalized with kAE1 at cell surface, whether wild-type proteins (Fig. 5*A*) or the different combinations of wild-type/mutant proteins (kAE1-F419A/L420A/D421A, delABS-RhBG, delABS-F419A/L420A/D421A; not shown) were analyzed. Using PLA, we revealed a clear interaction between the two proteins, in every configurations (*kAE1-RhBG* and *delABS-F419A/L420A/D421A*, Fig. 5*B*, *right panels*; kAE1-F419A/L420A/D421A and delABS-RhBG, not shown). As a control, no signal was detected in noninduced (*ni*) cells for kAE1 expression (Fig. 5*B*, *left panels*). Moreover, kAE1-ankyrin-G interaction was kept in the kAE1-RhBG cotransfectants, with (wild type) or without (F419A/L420A/D421A) RhBG binding to ankyrin-G (not shown). Likewise, RhBG was still interacting with ankyrin-G in the presence of wild-type kAE1 or kAE1-delABS (not shown). Altogether, these data

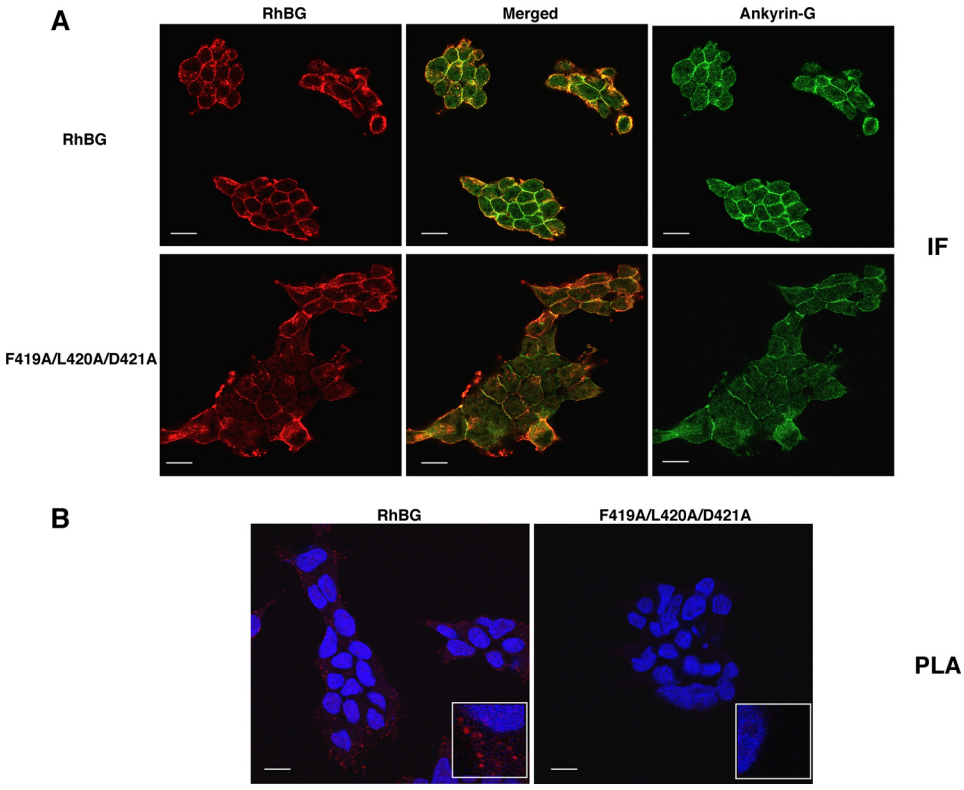

FIGURE 4. **Analysis of the interaction between RhBG and ankyrin-G by coimmunoprecipitation *in situ*.** *A*, colocalization of recombinant RhBG with endogenous ankyrin-G. HEK293 cells transfected with wild-type (*RhBG*) or mutant (*F419A/L420A/D421A*) RhBG cDNA were grown on poly-L-lysine coverslips, fixed, and permeabilized as in Fig. 2, stained with rabbit anti-RhBG (*RhBG*, *red*) and mouse anti-ankyrin-G (*Ankyrin-G*, *green*), then stained with Alexa Fluor 568 anti-rabbit and Alexa Fluor 488 anti-mouse IgG, respectively, and analyzed by confocal microscopy. *Merged*, overlay of RhBG and ankyrin-G immunofluorescence (*IF*) signals. *B*, interaction of RhBG with ankyrin-G. The same cells were treated and stained with primary antibodies as in *A* and then subjected to PLA analysis. Samples were mounted in ProLong Gold antifade reagent with DAPI, allowing cell nuclei staining. The *red* PLA signal was clearly visible in cells expressing wild-type RhBG and absent in those expressing RhBG-F419A/L420A/D421A. *Inset*, magnification (×16) of a selected region of PLA image. *Scale bars*, 15 μm.

show that RhBG and kAE1 are associated not only through their common binding to ankyrin-G but also by a direct interaction between them. RhBG-kAE1 association is independent of their ankyrin-G binding, and the interaction of one transmembrane protein with ankyrin-G is not affected by expression and ankyrin-G binding of the other.

Impact of kAE1 Expression on RhBG Expression and Activity in HEK293 Cells—Considering the above results, expression and NH_3 transport function of recombinant RhBG were tested in our inducible kAE1 expression system. Flow cytometry analysis of HEK293 cells cotransfected with kAE1 and RhBG cDNAs, wild-type or mutated on their ankyrin-G binding site, showed no main difference of wild-type RhBG or F419A/L420A/D421A mutant expression, when comparing each cell line in induced and noninduced kAE1 expression conditions (Table 1). Surface expression of RhBG-F419A/L420A/D421A protein was lower than that of wild-type RhBG, most probably because of the disruption of its anchorage to the membrane skeleton. Then NH_3 transport activity of RhBG was measured by stopped flow spectrofluorometry, using BCECF-AM as an intracellular fluorescent pH-sensitive probe in the presence of an inwardly directed 20 meq NH_4^+ gradient at 15 °C and pH 7.2, as described previously (2, 10). This temperature (instead of the more physiological 37 °C) was used because kinetics at 37 °C are too rapid (much <1 s) to precisely measure NH_3 transport. The time course of the fluorescence increase (proportional to intracellular pH increase as determined by a titration on HEK293 cells; see "Experimental Procedures") was recorded (Fig. 6) and allowed the calculation of alkalinization rate constants k (s^{-1}) (Table 1). Comparison of k values between noninduced (ni) and induced (i) conditions for each cell line revealed no significant difference (Mann-Whitney U test). These constants were then corrected taking into account the relative surface expression level of RhBG in each cell line as compared with cells expressing wild-type RhBG and noninduced for kAE1 expression (*kAE1 ni-RhBG*, *100%*), and by subtracting the passive diffusion constant of cells expressing kAE1 alone (*kAE1 i*) which was identical to that of noninduced (*kAE1 ni*) or nontransfected cells (Table 1, $k = 0.18 \pm 0.02\ s^{-1}$). Thus, transport efficiencies were comparable between HEK293 cells expressing RhBG without (ni) or with (i) simultaneous expression of wild-type kAE1 or delABS mutant (between 100 and 129%). Moreover, inhibition of NH_3 transport in cells expressing an RhBG protein deficient in ankyrin-G binding (RhBG-F419A/L420A/D421A) was not modified by kAE1 expression (between 8 and 13% of residual activity).

Cl^-/HCO_3^- Exchange Activity of Recombinant kAE1 in HEK293 Cells—Recently, we described the measurement of the rapid and specific Cl^-/HCO_3^- exchange by stably expressed eAE1 in HEK293 cells, using stopped flow spectrofluorometry (19). Likewise, we determined here the Cl^-/HCO_3^- exchange capacity of recombinant wild-type kAE1 or delABS mutant by

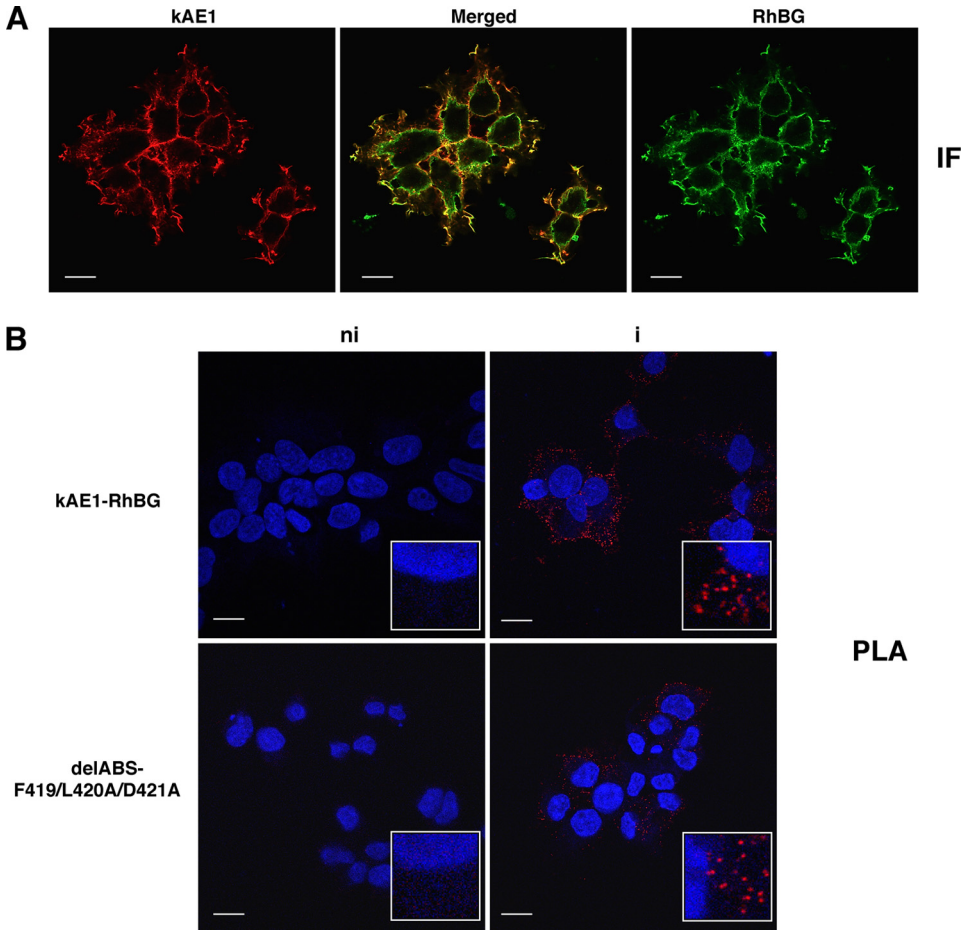

FIGURE 5. **Analysis of the interaction between RhBG and kAE1 by coimmunoprecipitation *in situ*.** *A*, colocalization of recombinant RhBG and kAE1. HEK293 cells, cotransfected with kAE1 and RhBG cDNAs, were grown on poly-L-lysine coverslips, tetracycline-induced for kAE1 expression, fixed, stained with rat BRAC17 anti-AE1 (*kAE1, red*) and mouse A-08 anti-RhBG (*RhBG, green*), then stained with Alexa Fluor 568 anti-rat and Alexa Fluor 488 anti-mouse IgG, respectively, and analyzed by confocal microscopy. *Merged*, overlay of kAE1 and RhBG immunofluorescence (*IF*) signals. *B*, interaction of RhBG with kAE1. The same cells were either tetracycline-induced (*i*) or noninduced (*ni*), fixed, stained with mouse A-08 and rat BRAC17 conjugated with minus PLA probe, and then subjected to PLA analysis. Samples were mounted in ProLong Gold antifade reagent with DAPI, allowing cell nuclei staining. The *red* PLA signal was clearly visible in cells coexpressing kAE1 and RhBG, wild-type (*kAE1-RhBG*), or mutant (*delABS-F419A/L420A/D421A*) and absent in noninduced cells. *Inset*, magnification (×16) of a selected region of PLA image. *Scale bars*, 15 μm.

TABLE 1

Cell surface expression and NH_3 transport activity of RhBG in HEK293 cells ± kAE1 expression

nt, nontransfected parental HEK293 cells; ni, cells not induced for kAE1 expression; i, cells induced for kAE1 expression.

Cell lines	Expression[a]	Alkalinization rate constants (k)[b]	Transport efficiency[c]
	%	s^{-1}	%
nt	0	0.18 ± 0.02 (3)	0
kAE1 ni	0	0.18 ± 0.02 (5)	0
kAE1 i	0	0.18 ± 0.02 (8)	0
kAE1 ni-RhBG	100	0.90 ± 0.10 (7)	100
kAE1 i-RhBG	98	0.93 ± 0.12 (8)	106
delABS ni-RhBG	95	1.06 ± 0.07 (4)	129
delABS i-RhBG	110	0.98 ± 0.09 (5)	101
kAE1 ni-F419A/L420A/D421A	85	0.26 ± 0.05 (5)	13
kAE1 i-F419A/L420A/D421A	71	0.22 ± 0.04 (3)	8
delABS ni-F419A/L420A/D421A	35	0.21 ± 0.01 (3)	12
delABS i-F419A/L420A/D421A	55	0.22 ± 0.02 (3)	10

[a] Relative values to mean fluorescence intensity for kAE1 ni-RhBG.
[b] The values are means ± S.D.; *n* values are in parentheses.
[c] Relative values of alkalinization rate constants corrected for membrane expression of RhBG in kAE1 ni-RhBG cell line and after subtraction of the passive diffusion constant (kAE1 ni).

this methodology, using BCECF-AM and in the presence of inwardly directed 10 meq HCO_3^-/CO_2 and outwardly directed 67.5 meq Cl^- gradients at 30 °C and pH 7.2. As mentioned above for RhBG activity, experiments were not performed at 37 °C, because anion exchange lasts <1 s at this temperature, precluding an accurate determination of alkalinization rate constants. Using these optimal thermal conditions (30 °C), we observed a fast intracellular alkalinization for cells expressing kAE1 (*kAE1 i*, $k = 0.25 \pm 0.03\ s^{-1}$) compared with parental or noninduced cells lacking kAE1 expression (*nt* and *kAE1 ni*, $k = 0.05 \pm 0.02$ and $0.04 \pm 0.02\ s^{-1}$, respectively) (Fig. 7, *A* and *B*). After incubation with the anion exchanger inhibitor DIDS, Cl^-/HCO_3^- exchange by kAE1 was reduced at the parental HEK293 cell level (Fig. 7, *A* and *B*, $k = 0.06 \pm 0.05\ s^{-1}$). HEK293 cells expressing kAE1-delABS (not binding to ankyrin-G) exhibited an alkalinization similar to noninduced or DIDS-treated wild-type kAE1 cells (Fig. 7, *A* and *B*, *delABS i*, $k = 0.06 \pm 0.02\ s^{-1}$), indicating that this mutant protein is not functional. Of note, a kAE1 mutant protein still bearing one of the three ankyrin-G binding sites, *i.e.* the amino acids 110–120 (major ankyrin-R binding site in eAE1 protein), exhibited the same characteristics as the delABS mutant: no detectable surface expression, no interaction with ankyrin-G in PLA, and no residual Cl^-/HCO_3^- exchange activity in HEK293 cells (not

shown). This result confirmed that these 11 residues constitute only a secondary ankyrin-G binding site in the kAE1 protein, as deduced from our yeast two-hybrid data.

Expression of Recombinant Wild-type and Mutant kAE1 in Polarized MDCK Cells—To validate the data from experiments in HEK293 cells, kAE1 expression was investigated in polarized epithelial MDCK cells. Because several attempts to obtain tetracycline-inducible expression of kAE1 after stable transfection have been unsuccessful, subconfluent MDCK cells were transiently transfected with wild-type or delABS mutant kAE1 cDNA, allowed to polarize for 4 days, labeled with rabbit anti-AE1 and mouse anti-ankyrin-G, and analyzed by immunofluorescence confocal microscopy (Fig. 8). Wild-type kAE1 (*red*, *left panels*) was properly expressed at the basolateral membrane (*XY* horizontal and *XZ* sections) as compared with ZO-1 staining (*green, bottom panel*) representative of the tight junctions and colocalized with endogenous basolateral ankyrin-G (*merged*, *second left panel*). In contrast, the delABS mutant exhibited an exclusive intracellular labeling indicating a total retention on cytoplasmic membranes (*red*, *right panels*) and did not colocalize with ankyrin-G (*merged*, *second right panel*). In polarized epithelial cells, the delABS protein is thus unable to anchor to the plasma membrane. These results, together with PLA data in HEK293 cells, constitute a strong evidence of a physical RhBG·kAE1·ankyrin-G complex in kidney epithelial cells.

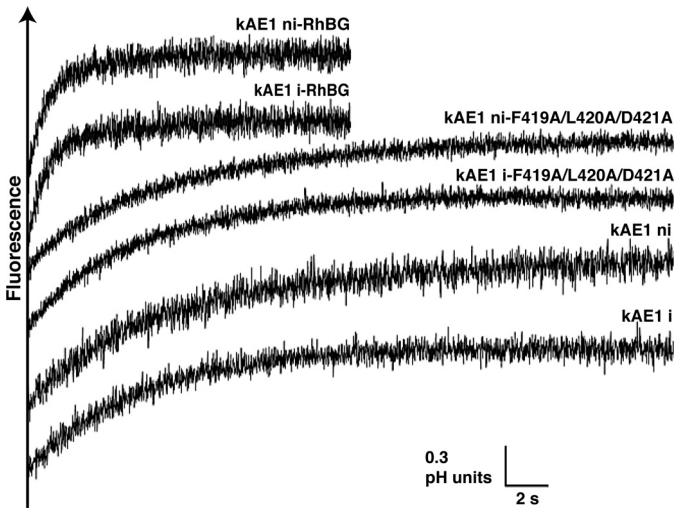

FIGURE 6. **Typical time course of fluorescence changes in HEK293 cells expressing RhBG, kAE1, or both proteins and exposed to ammonium gradients.** Cells loaded with the fluorescent pH-sensitive probe BCECF-AM were submitted to an inwardly directed 20 mEq NH_4^+ gradient at 15 °C. pH_i-dependent fluorescence changes were monitored using a stopped flow spectrofluorometer. Data from at least three time courses were averaged and fitted to a monoexponential function using the simplex procedure of Biokine software (Bio-Logic), from which alkalinization rate constants (k, s^{-1}) were determined. All experiments were repeated three to eight times to obtain the k values in Table 1. *ni* and *i*, noninduced and induced cells for kAE1 expression, respectively. delABS ni-RhBG, delABS i-RhBG, delABS ni-F419A/L420A/D421A, and delABS i-F419A/L420A/D421A (not shown) exhibited time courses similar to kAE1 ni-RhBG, kAE1 i-RhBG, kAE1 ni-F419A/L420A/D421A, and kAE1 i-F419A/L420A/D421A, respectively.

DISCUSSION

Up to now, the erythroid Rh·eAE1·ankyrin-R complex was considered not to have a counterpart in epithelial kidney cells. Indeed, although we have previously shown that RhBG interacts with ankyrin-G (1), it was generally assumed that kAE1 was not able to bind to this membrane adaptor protein because of a predicted altered structure of its truncated N terminus. In this study, we provided evidence that kAE1 actually binds not only to ankyrin-G but also to RhBG. This structural complex is also functional because interaction with ankyrin-G appears to be essential for the activity of its two transmembrane partners.

By yeast two-hybrid studies, we showed a direct interaction *in vitro* between the cytoplasmic N terminus of kAE1 and the D3-D4 repeat subdomains of the membrane binding domain of ankyrin-G. The D3-D4 domains of ankyrins associate with a number of membrane proteins, for example: Na^+,K^+-ATPase (26), voltage-gated sodium channels (27), nervous system cell adhesion molecules (28)), and particularly RhBG (1) and eAE1 (29). Of note, eAE1 has been shown to also interact with the D2 domain of ankyrin-R, and the region involved in this binding was located in the extreme N terminus of eAE1, which is actually lacking in kAE1 protein (*i.e.* amino acids 1–65) (29, 30). Mapping of ankyrin-G binding determinants in the N terminus

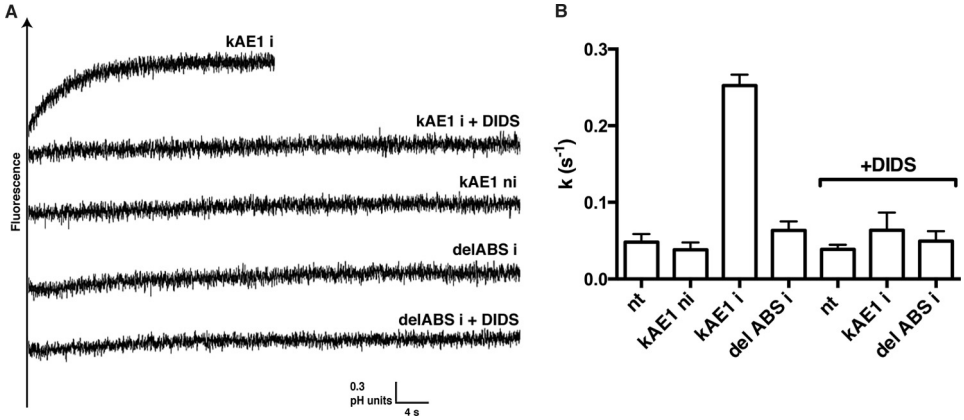

FIGURE 7. **Cl^-/HCO_3^- exchange activity in HEK293 cells expressing inducible kAE1 protein.** *A*, typical time course of fluorescence changes in recombinant HEK293 cells exposed to chloride and bicarbonate gradients. Cells loaded with the fluorescent pH-sensitive probe BCECF-AM were submitted to inwardly directed 10 mEq HCO_3^-/CO_2 and outwardly directed 67.5 mEq Cl^- gradients at 30 °C. pH_i-dependent fluorescence changes were monitored and analyzed as in Fig. 6. *B*, all experiments were repeated three to five times to obtain the values of alkalinization rate constants (k, s^{-1}). The values are means ± S.D. *nt*, nontransfected parental HEK293 cells. *ni* and *i*, noninduced or induced cells for kAE1 expression, respectively. + *DIDS*, cells incubated with the anion exchanger inhibitor DIDS (10 μM) for 30 min.

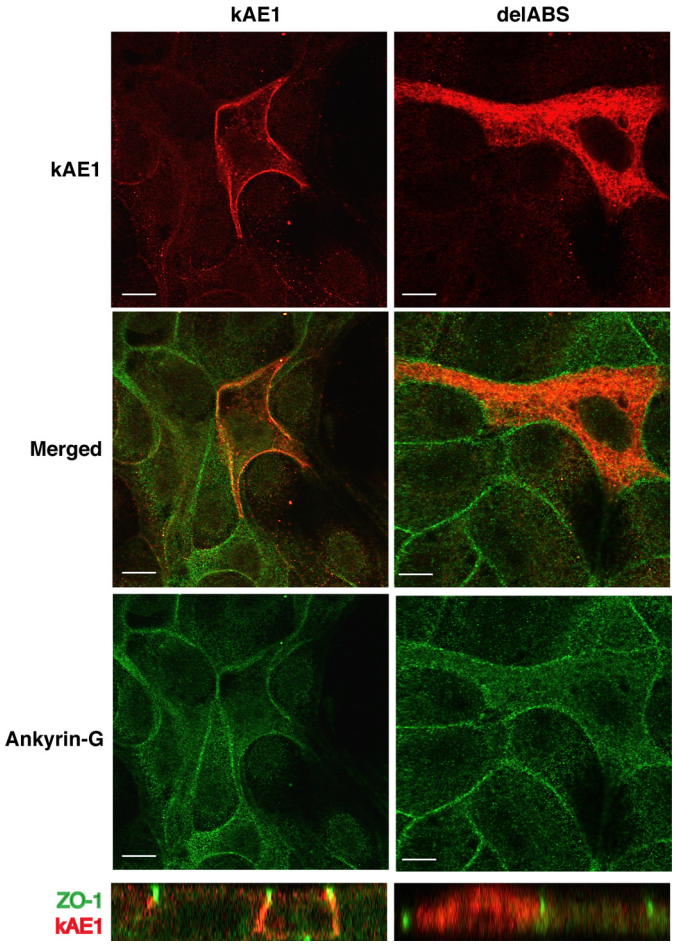

FIGURE 8. **Effect of disruption of the ankyrin-G-binding site on plasma membrane expression of kAE1.** MDCK cells were grown to subconfluency on poly-L-lysine coverslips, transiently transfected with wild-type or delABS mutant kAE1 cDNA, allowed to polarize for 4 days, fixed, permeabilized, stained with rabbit anti-AE1 (*kAE1*, *red*) and either mouse anti-ankyrin-G (*Ankyrin-G*, *green*) or mouse anti-ZO-1 (zonula occludens) conjugated to Alexa Fluor 488 (*ZO-1*, *green in XZ sections*), and then stained with either Alexa Fluor 568 anti-rabbit and Alexa Fluor 488 anti-mouse or Alexa Fluor 568 anti-rabbit IgG alone, respectively. *Top* and *center panels*, *XY* horizontal sections of wild-type (*kAE1*, *left*) and mutant (*delABS*, *right*) kAE1. *Merged*, overlay of kAE1 and ankyrin-G immunofluorescence signals. *Bottom panels*, *XZ* vertical sections allowing localization of kAE1 (*red*) with respect to tight junctions stained for ZO-1 (*green*). *Scale bars*, 5 μm.

of kAE1 revealed three dispersed regions including altogether ~100 amino acids. One of these stretches (residues 110–120) is identical to a major interacting loop (residues 175–185) of the cytoplasmic N terminus of eAE1 with ankyrin-R (21) but appears to be a secondary docking site for ankyrin-G in our two-hybrid experiments because its deletion alone has no effect on the binding efficiency. The two other interacting regions of kAE1 (residues 241–319 and 328–331) do not encompass any of the determinants defined for eAE1 (from amino acids 70–302 or 5–237 in eAE1 or kAE1 numberings, respectively) (31, 32). All three domains must be deleted or mutated for a complete inhibition of ankyrin-G binding. Crystallographic and other biophysical analyses suggested a different conformation of kAE1 cytoplasmic N terminus compared with that of eAE1 (16, 17, 21), which probably accounts for the very limited redundancy of ankyrin binding regions in the two proteins. Moreover, the three ankyrin species (R, B, and G) display 17% amino acid sequence divergence between their membrane binding domains (33), which should imply the involvement of different residues of ankyrin-G D3-D4 repeat subdomains in the interaction with kAE1 compared with ankyrin-R-eAE1 association (32). Sequence dissimilarities of ankyrins together with folding differences of AE1 N termini most probably explain the absence of interaction of kAE1 with ankyrin-R species (14, 15). Further detailed mutagenesis studies will help identify more precisely the interfacial contacts between kAE1 and ankyrin-G.

The kAE1-ankyrin-G interaction was confirmed and reinforced *ex vivo* by coimmunoprecipitation *in situ* (PLA) in HEK293 cells expressing endogenous ankyrin-G and recombinant kAE1 after tetracycline induction. PLA technology is fairly recent but has already been widely used for studying protein interaction (for review see Ref. 34). The HEK293 cell model was mainly used in our study because, despite many attempts, we could not establish an inducible kAE1 expression in stably transfected MDCK cells. Moreover, HEK293 cells have been proved to be a more accurate model than MDCK cells in functional studies using stopped flow spectrofluorometry (2, 10). The kAE1-delABS mutant was not detectable at the cell surface, but in immunofluorescence experiments using anti-cytoplasmic Nter antibody, this protein was revealed mainly on cytoplasmic structures and partly at the plasma membrane where it colocalized with endogenous ankyrin-G. These data suggest that kAE1-delABS can traffic, although inefficiently, to the plasma membrane. The negative PLA results obtained with this mutant may thus be considered as relevant to a disruption of interaction between its cytoplasmic N terminus and ankyrin-G. Importantly, the reliability of PLA data on kAE1 was strengthened by showing that the previously demonstrated interaction of RhBG with ankyrin-G (1) could be also evidenced here by PLA. RhBG and kAE1 are associated not only through their common interaction with ankyrin-G but also directly, as shown by PLA. Similarly, proteins of the erythroid Rh complex (Rh and RhAG) coimmunoprecipitate with eAE1 in the RBC membrane (4). We also observed that ankyrin-G binding to RhBG and/or kAE1 is not a prerequisite to their own association.

In our HEK293 cotransfectant cells, RhBG plasma membrane expression was not modulated by kAE1 coexpression. Thus, in a nonpolarized cell system, RhBG and kAE1 are most probably independently expressed and targeted to the plasma membrane. Previously, we proposed a model in which phosphorylation of Tyr^{429} in the C terminus of RhBG is essential for its targeting to the basolateral membrane of kidney epithelial cells, and then Tyr^{429} dephosphorylation allows anchoring of the protein to the underlying spectrin-based skeleton via ankyrin-G (2). Likewise, kAE1 basolateral membrane location in polarized MDCK cells has been shown to be controlled by reversible phosphorylation of two tyrosine residues of the protein, and the authors suggested that this regulation operates *in vivo* according to the systemic acid-base homeostasis (35). Moreover, our present data in this kidney epithelial cell model clearly showed that the kAE1-delABS mutant was exclusively retained on cytoplasmic structures, similarly to the RhBG-F419A/L420A/D421A mutant previously reported (1). We could therefore anticipate that RhBG and kAE1 are also inde-

pendently expressed in polarized α-intercalated cells, and their basolateral location at the plasma membrane is modulated by both their respective binding to ankyrin-G and phosphorylation status.

NH_3 transport activity of RhBG was not affected by coexpression of kAE1 in recombinant HEK293 cells. However, because both proteins directly interact *ex vivo* as demonstrated by coimmunoprecipitation *in situ* in these cells and also indirectly by their common binding to ankyrin-G, a functional modulation of RhBG by kAE1 in the basolateral domain of α-intercalated cells cannot be ruled out. Of note, CO_2, HCO_3^-, NH_3, and NH_4^+ are always present inside the cell *in vivo*; if the pH is changing, their respective concentrations are also modified, which modulates function of both RhBG and kAE1. An important finding is that RhBG (2) and possibly kAE1 need to associate with ankyrin-G to be functional. Previous reports demonstrated a similar link between ankyrin binding and activity of an ion channel: ankyrin-G for cardiac Nav1.5 and neuronal Nav1.6 sodium channels (36, 37) and ankyrin-B for cardiac K_{ATP} channel (38). A very recent study showed a physical and functional interaction between kAE1 and Na^+,K^+-ATPase in renal α-intercalated cells (39), and Na^+,K^+-ATPase is known to bind ankyrin-G (26). The renal RhBG·kAE1·ankyrin-G complex described here, possibly including Na^+,K^+-ATPase, is a new evidence of the great diversity of proteins that are organized in membrane microdomains in many cell types, under the control of ankyrins: ankyrin-G for neurofascin, KCNQ2/3, and voltage-gated Na^+ channel in epithelial cells (40–44) or E-cadherin and Na^+,K^+-ATPase in axon initial segment (33, 45) and ankyrin-B for Na^+,K^+-ATPase, Na^+-Ca^{2+} exchanger, and inositol triphosphate receptor in cardiomyocytes (46–48) and ankyrin-R for Rh and eAE1 in RBCs (4, 6). However, whereas extracellular epitopes of mutant RhBG-F419A/L420A/D421A are detectable at the surface of HEK293 cells (2), mutant kAE1-delABS is not, although it is partly expressed at plasma membrane. The inactivity of the kAE1 mutant might therefore be caused only indirectly by the absence of ankyrin-G binding, the main reason being an inefficient traffic and/or a conformational change of the protein induced by the mutations/deletions. This question will hopefully be solved when the ankyrin-G interaction site is determined more precisely and restricted to a less extended region of the N terminus, potentially leading to the use of a more correctly folded mutant protein in functional studies. Unfortunately, no murine model of renal ankyrin-G deficiency is available to further investigate *in vivo* the role of ankyrin-G binding on kAE1 expression and function. Anyway, such an animal model might not be informative because it has been reported that depletion of ankyrin-G in human bronchial epithelial cells by small interfering RNA resulted in a dramatic phenotype with loss of lateral plasma membrane and absence of proteins (Na^+,K^+-ATPase, β2-spectrin) that are normally localized in this membrane domain (49).

In conclusion, this study provides, for the first time, evidence that a molecular complex between the ammonium transporter RhBG, the anion exchanger kAE1, and the membrane adaptor ankyrin-G is present at the plasma membrane of kidney epithelial cells and abolishes the current paradigm for a direct anchoring of kAE1 to the cytoskeleton independently of ankyrin. The association of the three proteins is functional because RhBG and possibly kAE1 carry out their transport activity only when interacting with the spectrin-based skeleton through ankyrin-G. Future investigations will indicate whether the RhBG·kAE1·ankyrin-G complex could fulfill the functions of a metabolon that would participate in the regulation of acid/base homeostasis by excreting ammonium and protons in urine.

Acknowledgments—We thank Nicole Boggetto (Flow cytometry platform, Institut Jacques-Monod, Paris, France) for cell sorting experiments using a fluorescence-activated cell sorter Influx 500 (BD Biosciences), and Julien Picot and Sylvain Bigot (Institut National de la Transfusion Sanguine, Paris, France) for flow cytometry analysis. We also thank Dr. Wassim El Nemer (INSERM U1134) and Dr. Jean-Philippe Semblat (Institut National de la Transfusion Sanguine, Paris, France) for helpful advice on PLA experiments and immunofluorescence confocal microscopy, respectively.

REFERENCES

1. Lopez, C., Métral, S., Eladari, D., Drevensek, S., Gane, P., Chambrey, R., Bennett, V., Cartron, J. P., Le Van Kim, C., and Colin, Y. (2005) The ammonium transporter RhBG: requirement of a tyrosine-based signal and ankyrin-G for basolateral targeting and membrane anchorage in polarized kidney epithelial cells. *J. Biol. Chem.* **280,** 8221–8228
2. Sohet, F., Colin, Y., Genetet, S., Ripoche, P., Métral, S., Le Van Kim, C., and Lopez, C. (2008) Phosphorylation and ankyrin-G binding of the C-terminal domain regulate targeting and function of the ammonium transporter RhBG. *J. Biol. Chem.* **283,** 26557–26567
3. Alper, S. L. (2009) Molecular physiology and genetics of Na^+-independent SLC4 anion exchangers. *J. Exp. Biol.* **212,** 1672–1683
4. Bruce, L. J., Beckmann, R., Ribeiro, M. L., Peters, L. L., Chasis, J. A., Delaunay, J., Mohandas, N., Anstee, D. J., and Tanner, M. J. (2003) A band 3-based macrocomplex of integral and peripheral proteins in the RBC membrane. *Blood* **101,** 4180–4188
5. Ripoche, P., Bertrand, O., Gane, P., Birkenmeier, C., Colin, Y., and Cartron, J. P. (2004) Human Rhesus-associated glycoprotein mediates facilitated transport of NH_3 into red blood cells. *Proc. Natl. Acad. Sci. U.S.A.* **101,** 17222–17227
6. Nicolas, V., Le Van Kim, C., Gane, P., Birkenmeier, C., Cartron, J. P., Colin, Y., and Mouro-Chanteloup, I. (2003) Rh-RhAG/ankyrin-R, a new interaction site between the membrane bilayer and the red cell skeleton, is impaired by Rh(null)-associated mutation. *J. Biol. Chem.* **278,** 25526–25533
7. Brosius, F. C., 3rd, Alper, S. L., Garcia, A. M., and Lodish, H. F. (1989) The major kidney band 3 gene transcript predicts an amino-terminal truncated band 3 polypeptide. *J. Biol. Chem.* **264,** 7784–7787
8. Alper, S. L., Natale, J., Gluck, S., Lodish, H. F., and Brown, D. (1989) Subtypes of intercalated cells in rat kidney collecting duct defined by antibodies against erythroid band 3 and renal vacuolar H^+-ATPase. *Proc. Natl. Acad. Sci. U.S.A.* **86,** 5429–5433
9. Verlander, J. W., Miller, R. T., Frank, A. E., Royaux, I. E., Kim, Y. H., and Weiner, I. D. (2003) Localization of the ammonium transporter proteins RhBG and RhCG in mouse kidney. *Am. J. Physiol. Renal Physiol.* **284,** F323–F337
10. Zidi-Yahiaoui, N., Mouro-Chanteloup, I., D'Ambrosio, A. M., Lopez, C., Gane, P., Le van Kim, C., Cartron, J. P., Colin, Y., and Ripoche, P. (2005) Human Rhesus B and Rhesus C glycoproteins: properties of facilitated ammonium transport in recombinant kidney cells. *Biochem. J.* **391,** 33–40
11. Liu, Z., Peng, J., Mo, R., Hui, C., and Huang, C. H. (2001) Rh type B glycoprotein is a new member of the Rh superfamily and a putative ammonia transporter in mammals. *J. Biol. Chem.* **276,** 1424–1433
12. Bennett, V., and Baines, A. J. (2001) Spectrin and ankyrin-based pathways: metazoan inventions for integrating cells into tissues. *Physiol. Rev.* **81,** 1353–1392
13. Mohler, P. J., Gramolini, A. O., and Bennett, V. (2002) Ankyrins. *J. Cell Sci.*

115, 1565–1566
14. Ding, Y., Casey, J. R., and Kopito, R. R. (1994) The major kidney AE1 isoform does not bind ankyrin (Ank1) *in vitro*: an essential role for the 79 NH_2-terminal amino acid residues of band 3. *J. Biol. Chem.* **269,** 32201–32208
15. Wang, C. C., Moriyama, R., Lombardo, C. R., and Low, P. S. (1995) Partial characterization of the cytoplasmic domain of human kidney band 3. *J. Biol. Chem.* **270,** 17892–17897
16. Zhang, D., Kiyatkin, A., Bolin, J. T., and Low, P. S. (2000) Crystallographic structure and functional interpretation of the cytoplasmic domain of erythrocyte membrane band 3. *Blood* **96,** 2925–2933
17. Pang, A. J., Bustos, S. P., and Reithmeier, R. A. (2008) Structural characterization of the cytosolic domain of kidney chloride/bicarbonate anion exchanger 1 (kAE1). *Biochemistry* **47,** 4510–4517
18. Quentin, F., Eladari, D., Cheval, L., Lopez, C., Goossens, D., Colin, Y., Cartron, J. P., Paillard, M., and Chambrey, R. (2003) RhBG and RhCG, the putative ammonia transporters, are expressed in the same cells in the distal nephron. *J. Am. Soc. Nephrol.* **14,** 545–554
19. Frumence, E., Genetet, S., Ripoche, P., Iolascon, A., Andolfo, I., Le Van Kim, C., Colin, Y., Mouro-Chanteloup, I., and Lopez, C. (2013) Rapid Cl^-/HCO_3^- exchange kinetics of AE1 in HEK293 cells and hereditary stomatocytosis red blood cells. *Am. J. Physiol. Cell Physiol.* **305,** C654–C662
20. Laemmli, U. K. (1970) Cleavage of structural proteins during the assembly of the head of bacteriophage T4. *Nature* **227,** 680–685
21. Chang, S. H., and Low, P. S. (2003) Identification of a critical ankyrin-binding loop on the cytoplasmic domain of erythrocyte membrane band 3 by crystal structure analysis and site-directed mutagenesis. *J. Biol. Chem.* **278,** 6879–6884
22. Bustos, S. P., and Reithmeier, R. A. (2011) Protein 4.2 interaction with hereditary spherocytosis mutants of the cytoplasmic domain of human anion exchanger 1. *Biochem. J.* **433,** 313–322
23. Cordat, E., Kittanakom, S., Yenchitsomanus, P. T., Li, J., Du, K., Lukacs, G. L., and Reithmeier, R. A. (2006) Dominant and recessive distal renal tubular acidosis mutations of kidney anion exchanger 1 induce distinct trafficking defects in MDCK cells. *Traffic* **7,** 117–128
24. Toye, A. M., Banting, G., and Tanner, M. J. (2004) Regions of human kidney anion exchanger 1 (kAE1) required for basolateral targeting of kAE1 in polarised kidney cells: mis-targeting explains dominant renal tubular acidosis (dRTA). *J. Cell Sci.* **117,** 1399–1410
25. Söderberg, O., Gullberg, M., Jarvius, M., Ridderstråle, K., Leuchowius, K. J., Jarvius, J., Wester, K., Hydbring, P., Bahram, F., Larsson, L. G., and Landegren, U. (2006) Direct observation of individual endogenous protein complexes in situ by proximity ligation. *Nat. Methods* **3,** 995–1000
26. Thevananther, S., Kolli, A. H., and Devarajan, P. (1998) Identification of a novel ankyrin isoform (AnkG190) in kidney and lung that associates with the plasma membrane and binds alpha-Na, K-ATPase. *J. Biol. Chem.* **273,** 23952–23958
27. Srinivasan, Y., Lewallen, M., and Angelides, K. J. (1992) Mapping the binding site on ankyrin for the voltage-dependent sodium channel from brain. *J. Biol. Chem.* **267,** 7483–7489
28. Davis, J. Q., and Bennett, V. (1994) Ankyrin binding activity shared by the neurofascin/L1/NrCAM family of nervous system cell adhesion molecules. *J. Biol. Chem.* **269,** 27163–27166
29. Michaely, P., and Bennett, V. (1995) The ANK repeats of erythrocyte ankyrin form two distinct but cooperative binding sites for the erythrocyte anion exchanger. *J. Biol. Chem.* **270,** 22050–22057
30. Michaely, P., Tomchick, D. R., Machius, M., and Anderson, R. G. (2002) Crystal structure of a 12 ANK repeat stack from human ankyrinR. *EMBO J.* **21,** 6387–6396
31. Kim, S., Brandon, S., Zhou, Z., Cobb, C. E., Edwards, S. J., Moth, C. W., Parry, C. S., Smith, J. A., Lybrand, T. P., Hustedt, E. J., and Beth, A. H. (2011) Determination of structural models of the complex between the cytoplasmic domain of erythrocyte band 3 and ankyrin-R repeats 13–24. *J. Biol. Chem.* **286,** 20746–20757
32. Grey, J. L., Kodippili, G. C., Simon, K., and Low, P. S. (2012) Identification of contact sites between ankyrin and band 3 in the human erythrocyte membrane. *Biochemistry* **51,** 6838–6846
33. Bennett, V., and Healy, J. (2008) Organizing the fluid membrane bilayer: diseases linked to spectrin and ankyrin. *Trends Mol. Med.* **14,** 28–36
34. Koos, B., Andersson, L., Clausson, C. M., Grannas, K., Klaesson, A., Cane, G., and Söderberg, O. (2014) Analysis of protein interactions in situ by proximity ligation assays. *Curr. Top. Microbiol. Immunol.* **377,** 111–126
35. Williamson, R. C., Brown, A. C., Mawby, W. J., and Toye, A. M. (2008) Human kidney anion exchanger 1 localisation in MDCK cells is controlled by the phosphorylation status of two critical tyrosines. *J. Cell Sci.* **121,** 3422–3432
36. Mohler, P. J., Rivolta, I., Napolitano, C., LeMaillet, G., Lambert, S., Priori, S. G., and Bennett, V. (2004) Nav1.5 E1053K mutation causing Brugada syndrome blocks binding to ankyrin-G and expression of Nav1.5 on the surface of cardiomyocytes. *Proc. Natl. Acad. Sci. U.S.A.* **101,** 17533–17538
37. Shirahata, E., Iwasaki, H., Takagi, M., Lin, C., Bennett, V., Okamura, Y., and Hayasaka, K. (2006) Ankyrin-G regulates inactivation gating of the neuronal sodium channel, Nav1.6. *J. Neurophysiol.* **96,** 1347–1357
38. Li, J., Kline, C. F., Hund, T. J., Anderson, M. E., and Mohler, P. J. (2010) Ankyrin-B regulates Kir6.2 membrane expression and function in heart. *J. Biol. Chem.* **285,** 28723–28730
39. Su, Y., Al-Lamki, R. S., Blake-Palmer, K. G., Best, A., Golder, Z. J., Zhou, A., and Karet Frankl, F. E. (2015) Physical and functional links between anion exchanger-1 and sodium pump. *J. Am. Soc. Nephrol.* **26,** 400–409
40. Zhou, D., Lambert, S., Malen, P. L., Carpenter, S., Boland, L. M., and Bennett, V. (1998) AnkyrinG is required for clustering of voltage-gated Na channels at axon initial segments and for normal action potential firing. *J. Cell Biol.* **143,** 1295–1304
41. Jenkins, S. M., and Bennett, V. (2001) Ankyrin-G coordinates assembly of the spectrin-based membrane skeleton, voltage-gated sodium channels, and L1 CAMs at Purkinje neuron initial segments. *J. Cell Biol.* **155,** 739–746
42. Pan, Z., Kao, T., Horvath, Z., Lemos, J., Sul, J. Y., Cranstoun, S. D., Bennett, V., Scherer, S. S., and Cooper, E. C. (2006) A common ankyrin-G-based mechanism retains KCNQ and NaV channels at electrically active domains of the axon. *J. Neurosci.* **26,** 2599–2613
43. Chung, H. J., Jan, Y. N., and Jan, L. Y. (2006) Polarized axonal surface expression of neuronal KCNQ channels is mediated by multiple signals in the KCNQ2 and KCNQ3 C-terminal domains. *Proc. Natl. Acad. Sci. U.S.A.* **103,** 8870–8875
44. Rasmussen, H. B., Frøkjaer-Jensen, C., Jensen, C. S., Jensen, H. S., Jørgensen, N. K., Misonou, H., Trimmer, J. S., Olesen, S. P., and Schmitt, N. (2007) Requirement of subunit co-assembly and ankyrin-G for M-channel localization at the axon initial segment. *J. Cell Sci.* **120,** 953–963
45. Kizhatil, K., Davis, J. Q., Davis, L., Hoffman, J., Hogan, B. L., and Bennett, V. (2007) Ankyrin-G is a molecular partner of E-cadherin in epithelial cells and early embryos. *J. Biol. Chem.* **282,** 26552–26561
46. Mohler, P. J., Schott, J. J., Gramolini, A. O., Dilly, K. W., Guatimosim, S., duBell, W. H., Song, L. S., Haurogné, K., Kyndt, F., Ali, M. E., Rogers, T. B., Lederer, W. J., Escande, D., Le Marec, H., and Bennett, V. (2003) Ankyrin-B mutation causes type 4 long-QT cardiac arrhythmia and sudden cardiac death. *Nature* **421,** 634–639
47. Mohler, P. J., Splawski, I., Napolitano, C., Bottelli, G., Sharpe, L., Timothy, K., Priori, S. G., Keating, M. T., and Bennett, V. (2004) A cardiac arrhythmia syndrome caused by loss of ankyrin-B function. *Proc. Natl. Acad. Sci. U.S.A.* **101,** 9137–9142
48. Mohler, P. J., Davis, J. Q., and Bennett, V. (2005) Ankyrin-B coordinates the Na/K ATPase, Na/Ca exchanger, and InsP3 receptor in a cardiac T-tubule/SR microdomain. *PLoS Biol.* **3,** e423
49. Kizhatil, K., and Bennett, V. (2004) Lateral membrane biogenesis in human bronchial epithelial cells requires 190-kDa ankyrin-G. *J. Biol. Chem.* **279,** 16706–16714
50. Li, B., and Fields, S. (1993) Identification of mutations in p53 that affect its binding to SV40 large T antigen by using the yeast two-hybrid system. *FASEB J.* **7,** 957–963
51. Bartel, P., Chien, C. T., Sternglanz, R., and Fields, S. (1993) Elimination of false positives that arise in using the two-hybrid system. *BioTechniques* **14,** 920–924